Comparison of Adapter Characterization Methods

J. Randa, *Senior Member, IEEE,* Wojciech Wiatr, *Member, IEEE,* and Robert L. Billinger

Abstract—We review and compare three different methods for characterization of precision adapters. Two of the methods are one-port techniques using two different reflective terminations in the one case and a matched load and multiple lines with reflective terminations in the other. The third technique is a conventional two-port adapter-removal technique. The intrinsic efficiencies of several different adapters are measured with each technique, and the results are compared. The results usually agree within about 0.005 for efficiencies near one. In all cases, the differences are consistent with the estimated uncertainties of the techniques, which range from about 0.002 to about 0.012, depending on the method, connectors, and frequency.

Index Terms—Adapter characterization, microwave adapters, microwave measurements, microwave transitions.

I. INTRODUCTION

AVAILABILITY of precision adapters greatly increases the versatility of measurement systems, permitting measurement of a device whose connector does not match that of the system. The use of adapters, however, generally requires that they be characterized to enable the user to correct for their effect. Accurate characterization of adapters remains a difficult task. As coaxial lines are pushed to ever higher frequencies (and higher waveguide bands), and the use of adapters increases, it becomes increasingly important to have reliable automated broad-band methods for adapter characterization. Methods using a vector network analyzer (VNA) meet these needs.

In this paper, we consider three different VNA-based techniques for characterizing adapters and compare their results for four representative adapters. An abbreviated summary of the work was presented in [1]. The present paper expands the discussion of the three methods, addresses the issue of reference plane location, provides analyses of the uncertainties, and presents additional results. The three methods treated comprise a one-port reflective-termination (RT) technique developed by Daywitt [2], [3], a multiline one-port (ML1P) method developed by Wiatr [4], [5], and the two-port adapter removal (AR) technique described in the documentation [6] for the VNA that was used in the measurements. Each method will be described, and their results compared. Since the RT technique does not determine the full scattering matrix and because our principal interest is in the use of adapters in noise and power
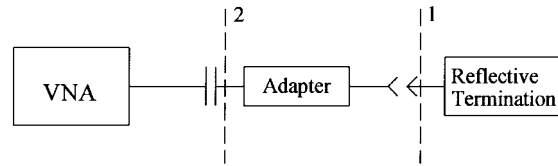
Fig. 1. Measurement configuration for the RT method.

measurements, the quantity that we choose for our comparison is the intrinsic efficiency of the adapter from plane 1 to plane 2, defined by

$$\eta_{21_0} = \frac{|S_{21}|^2}{1 - |S_{11}|^2}. \tag{1}$$

In noise measurements through adapters, the adapter efficiency is a crucial parameter. For a typical high-temperature noise source, a difference of 0.01 in adapter efficiency results in a difference of (approximately) 1% in the noise temperature.

In the following section, we review each of the three methods, estimate the measurement uncertainties, and discuss the location of the reference planes in each. Section III presents and compares the results of the measurements on several adapters using each of the three characterization methods. Conclusions are presented in Section IV.

II. REVIEW OF METHODS

A. RT Method

In the RT method [2], [3], one port of the adapter is connected to a calibrated port of the VNA, and the other port is terminated in a reflective load, as shown in Fig. 1. The reflection coefficient of the adapter and load is measured at reference plane 2, and the process is repeated with the reflective load replaced by a second reflective load, whose reflection coefficient differs in phase from that of the first by π. In practice, the reflective terminations are typically an offset short and an offset open for a coaxial port and a flush short and an offset short for a waveguide port. The relation between the reflection coefficient measured at reference plane 2 in Fig. 1 and the intrinsic efficiency of the adapter was derived in [3]. Assuming a reciprocal, low-loss adapter

$$|\Gamma_2| \approx \eta_{21_0}|\Gamma_{\rm rt}| - |\chi| \cos\phi$$
$$\chi \approx S_{22}(1 - \eta_{21_0}) \tag{2}$$

where $\Gamma_{\rm rt}$ is the reflection coefficient of the reflective termination ($|\Gamma_{\rm rt}| \approx 1$), and ϕ is a phase angle that varies (approximately) linearly and relatively rapidly (compared to η_{21_0}) with frequency. Equation (2) indicates that $|\Gamma_2|$ consists
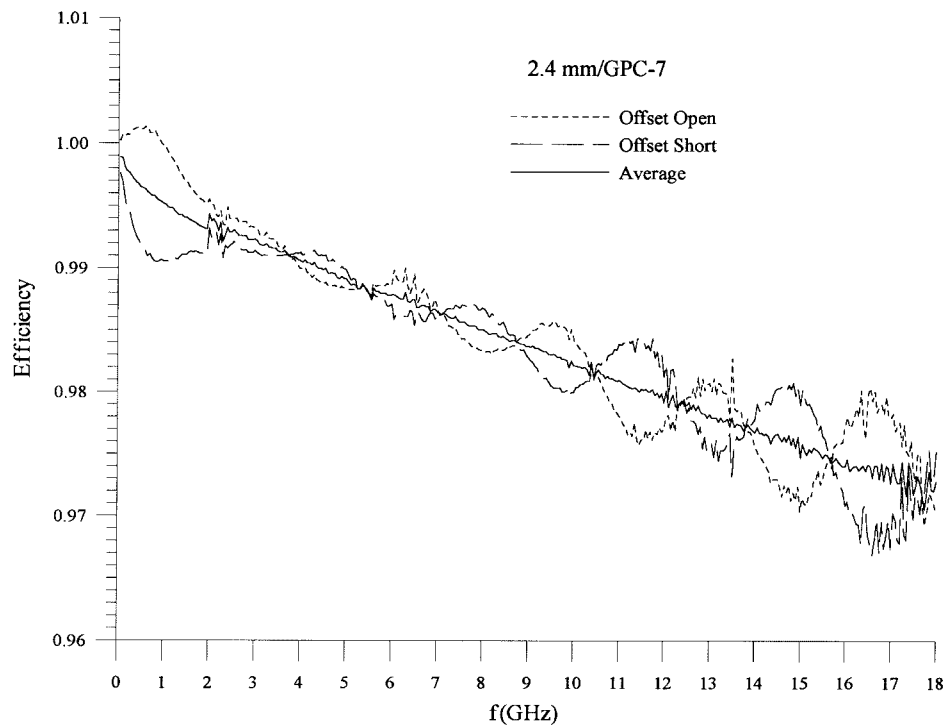
Fig. 2. Efficiency (solid line) as determined in the RT method.

of a rapidly varying piece $(|\chi|\cos\phi)$, due to reflection from the transition in the adapter, superimposed on a more slowly varying term $(\eta_{21_0}|\Gamma_{\mathrm{rt}}|)$, due to transmission through the adapter and reflection from the termination. The idea is then to measure $|\Gamma_2|$ and take an envelope average to remove the oscillations in frequency. That should yield $\eta_{21_0}|\Gamma_{\mathrm{rt}}|$, which can be divided by $|\Gamma_{\mathrm{rt}}|$ to yield the desired quantity. For a good flush short, $|\Gamma_{\mathrm{rt}}|$ can be taken to be one; but for an offset short or offset open, a correction is required to account for the loss in the small length of line constituting the offset.

The process of eliminating the oscillations in frequency is facilitated by measuring $|\Gamma_2|$ with two different reflective terminations, whose reflection coefficients differ in phase by π. Typical choices would be a flush short and an offset short for a waveguide port, or an offset open and an offset short for a coaxial port. As an example, we consider evaluation of an adapter from a 2.4-mm coaxial line to GPC-7 coaxial line. Referring to Fig. 1, we identify port 1 with the 2.4-mm port and port 2 with the GPC-7 port. We measured $|\Gamma_2|$, the reflection coefficient from port 2, when port 1 was terminated with two different reflective loads, in this case, an offset open and offset short. Each measured curve was then divided by $|\Gamma_{\mathrm{rt}}|$ to correct for the loss in the offset. The results are shown in the two dashed curves of Fig. 2. Each curve is approximately what would be expected from (2), regular oscillations $(|\chi|\cos\phi)$ on a smooth overall frequency dependence $(\eta_{21_0}|\Gamma_{\mathrm{rt}}|)$. The oscillations are out of phase because ϕ is different in the two cases.

To determine η_{21_0}, we average the two corrected curves and fit a smooth curve to the average. In principle, it would be sufficient to take the envelope average of just one of the curves [2], but using both curves facilitates the averaging and

also provides a check. The solid curve in Fig. 2 is the average of the two corrected curves. In actual applications a smooth fit to the average is used for η_{21_0}, but in the present comparison, we use the unsmoothed average since smoothing is not applied to the other methods. In noise-measurement applications [3], [7], further approximations are made to obtain the available power ratio α_{21}, defined as the available power at plane 2 divided by the available power at plane 1. For the current comparison, however, we are interested only in η_{21_0}.

A detail that should be addressed is the location of the reference plane and the connector joint loss [3], [8], [9] in this method. The VNA is calibrated in a conventional manner, and consequently reference plane 2 is at the junction of the two connectors. The standards used in the calibration are modeled with no joint loss in the connection. Consequently, if there is a significant repeatable loss in the connector joint, it is included in the VNA; it is not included in the properties of the adapter. Variations in the connection for different connectors of the same type or for repeated connections of the same pair of connectors are included in the uncertainties discussed below. The reflective termination attached to the other port of the adapter is modeled with no connector loss. Consequently, any loss in the connector joint at plane 1 is included in the adapter. Thus, the reference planes in Fig. 1 are shown slightly to the side of each connector junction, indicating where the effect of the joint loss is included. This inclusion of one joint loss, but not the other, in the adapter efficiency is actually well suited to the manner in which the adapters are used by the National Institute of Standards and Technology (NIST) Noise Project, as indicated in Fig. 3. The joint loss at plane 2 is included in the radiometer by the calibration process, whereas the joint loss at plane 1
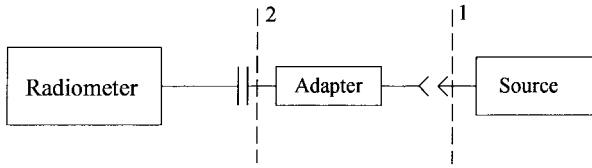
Fig. 3. Measurement configuration for noise-temperature measurement through an adapter.

Fig. 4. (a) Configuration for first calibration in ML1P method. (b) Configuration for second calibration in ML1P method.

is included in the adapter, so that the noise temperature of the source is measured immediately before the junction. This means that in the characterization of the adapter, care must be taken to measure it in the same orientation in which it will be used, with the side that will be connected to the radiometer connected to the VNA in the characterization measurements.

The feature of inclusion of one joint loss, but not the other, in the adapter characteristics is a natural feature of one-port characterization methods. If the standards at planes 1 and 2 in Fig. 1 are modeled in the same manner, the joint loss will be on the same side (left- or right-hand) for each reference plane, and therefore one joint loss will be part of the adapter and one will not. To do it differently in a one-port characterization would require either different modeling of the standards at the two reference planes or a measurement (or estimation) of the joint loss and correction for its effect.

The uncertainties in this method were treated most recently in [7], which identified three contributions to the uncertainty in η_{21_0}: the determination of the smoothed curve, the VNA measurement, and the connector variability (from connector to connector and from connection to connection with the same pair of connectors). The smoothed curve can generally be determined to 0.001 or less (for the standard, or one-sigma, uncertainty). The uncertainty in the VNA measurement is taken from the manufacturer's specifications. It depends on the calibration technique, frequency, and connector at plane 2, typically falling in the range 0.002 (GPC-7) to 0.012 (precision Type N at 18 GHz). It would be larger for 3.5- and 2.4-mm connectors, but they usually occur at plane 1 rather than plane 2. Connector variability refers to the connector at plane 1; variability of the connector at plane 2 is included in the VNA uncertainty. Conservative estimates inferred from the results of [10] are 0.001 for waveguide and most precision coaxial connectors, 0.002 for precision Type N. Reference [7] ignored any uncertainty arising from imperfections in the reflective terminations used in the measurements. The determination of η_{21_0} is sensitive to the magnitude, but not the phase of Γ_{rt}, and the uncertainty due to imperfect reflecting terminations is typically negligible $(\sim 5 \times 10^{-4})$ if calibration quality terminations are used. Combining the individual components results in a combined standard (1σ) uncertainty [11], [12] of about 0.003–0.005 in typical cases. In determining the *in situ* efficiency η_{21} [3], [7], which depends on the reflection coefficient of the load, there is an additional uncertainty due to the difference between η_{21} and η_{21_0}. Since our present comparison is for η_{21_0}, we can ignore that complication.
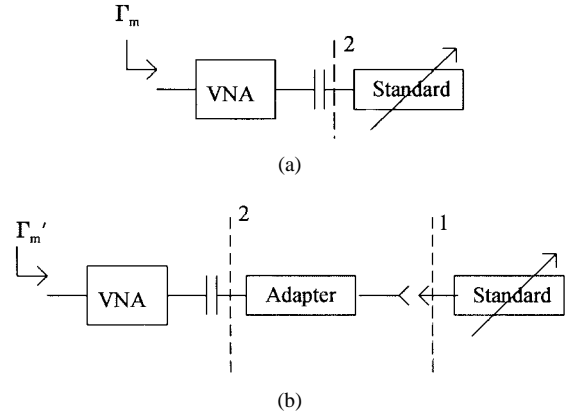
B. ML1P Method

Characterization of an adapter using the ML1P method [4], [5] begins with a calibration of the VNA at plane 2 using a matched load and several lines of differing lengths with reflective terminations [see Fig. 4(a)]. This is followed by a similar calibration at plane 1 with the adapter attached to the VNA, as shown in Fig. 4(b). From these two calibrations, the ML1P method determines the full scattering matrix of the adapter if we assume a reciprocal adapter. It also employs a mathematical transform of the reflection-coefficient measurements to provide a convenient framework for processing, discussing, and understanding the data.

Throughout this subsection, we shall use the subscript m to indicate a quantity measured at a reference plane within the VNA, so that the VNA's error box intervenes between Γ_m and the "true" Γ. The framework for the calibration rests on a bilinear transformation of a measured reflection coefficient Γ_m referenced to the measured reflection coefficient Γ_{ml} of a matched load ($\Gamma_l = 0$)

$$w(\Gamma_m) = \frac{1 - \Gamma_m \Gamma_{ml}^*}{\Gamma_m - \Gamma_{ml}}. \tag{3}$$

The actual reflection coefficient Γ is then related to $w(\Gamma_m)$ by [4]

$$w(\Gamma_m) = w_c + \frac{w_r}{\Gamma}$$
$$\Gamma = \frac{w_r}{w(\Gamma_m) - w_c} \tag{4}$$

where w_c and w_r are parameters determined in the calibration. In the complex w plane, w_c is interpreted as the position of the center of circles $|\Gamma| = \text{const}$, and w_r is interpreted as the radius of the circle $|\Gamma| = 1$.

The calibration procedure determines the three complex constants Γ_{ml}, w_c, and w_r. Γ_{ml} can be determined either directly from a measurement on a single standard matched load or from a series of measurements on a sliding load. The procedure for determining the constants w_c and w_r is best understood by referring to Fig. 5. It uses a set of lines of different length terminated in highly reflective loads. The simplest way to achieve this is to use a sliding short, and in our discussion we assume a sliding short is used. The reflection
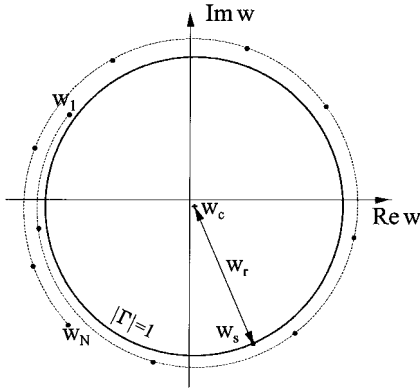
Fig. 5.   Representation of w plane for ML1P calibration.

coefficient of the sliding short is measured for a series ($i = 1, 2, \cdots, N$) of positions of the short. The sliding short is modeled by

$$\Gamma_i = \Gamma_r e^{-2\gamma l_i} \tag{5}$$

where Γ_r is the reflection coefficient in the reference position, γ is the propagation constant of the line along which the short slides, and l_i is the length of line from the reference position to the short when it is in the ith position. From (4), the corresponding w_i's are given by

$$w_i = w(\Gamma_i) = w_c + w_p e^{2\gamma l_i} \tag{6}$$

where $w_p = w_r / \Gamma_r$. The measured w_i lie (approximately) on a spiral in the w plane, as indicated by the points in Fig. 5. A fit of the measured $w(\Gamma_{mi})$ to (6) then determines the complex parameters w_c and w_p, as well as the parameters of the sliding short (Γ_r and γl_i). The fitting routine is detailed in [4]. A measurement of a standard flush short is used to provide a point on the $|\Gamma| = 1$ circle. This point is labeled $w_s = w(\Gamma_{ms})$. The radius w_r is given by

$$w_r = w_c - w_s. \tag{7}$$

To use this method to characterize an adapter, we first calibrate the VNA at plane 2 in Fig. 4(a), yielding the parameters Γ_{ml}, w_c, and w_r. The adapter is then connected to the VNA port, and a calibration is performed at the adapter output [plane 1 in Fig. 4(b)]. Quantities associated with this second calibration are labeled with primes, and the calibration constants are thus Γ'_{ml}, w'_c, and w'_r. The full scattering matrix of the adapter can be determined by this process if we assume a reciprocal adapter. The intrinsic efficiency is given by

$$\eta_{12_0} = \left| \frac{w_r}{w'_r} \right| \frac{(1 - |\Gamma_n|^2)}{|1 - w_c \Gamma_n|^2 - |w_r \Gamma_n|^2}$$

$$\Gamma_n \equiv \frac{\Gamma'_{ml} - \Gamma_{ml}}{1 - \Gamma'_{ml} \Gamma^*_{ml}}. \tag{8}$$

We write the equation for η_{12_0} rather than for η_{21_0} because it is much simpler, and the two are numerically indistinguishable in all our measurements.

To estimate the uncertainty in the intrinsic efficiency, we make the simplifying assumption that the effect of the VNA box in Fig. 4 is small. In practice, this can always be achieved

by performing a "precalibration" of the VNA before performing the first ML1P calibration, that is, perform a normal calibration at plane 2, followed by the ML1P calibration at plane 2, followed by the ML1P calibration at plane 1. Such a precalibration simplifies the uncertainty analysis, but it increases the measurement effort. In our comparison measurements, a precalibration was performed in some cases and not in others. For cases when the VNA is not precalibrated, the uncertainty could be somewhat larger than our current estimates, but we do not expect a very great increase. If the effect of the VNA box is small, then in the ML1P measurements w_r and w'_r will be near one in magnitude, and w_c, Γ_{ml}, Γ'_{ml}, and Γ_n will all be small. These approximations are not used in the actual evaluation of the efficiency, but they do simplify the uncertainty analysis.

The uncertainty in the intrinsic efficiency is given by

$$u(\eta_{21_0}) = \sqrt{u(w_r)^2 + u(w'_r)^2 + u(F)^2} \tag{9}$$

where F represents the second fraction in (8) and where we neglect correlations between uncertainties in F and those in w_r and w'_r. If we expand F and keep terms only through the lowest nonvanishing order in small quantities, we get

$$F \equiv \frac{1 - |\Gamma_n|^2}{|1 - w_c \Gamma_n|^2 - |w_r \Gamma_n|^2}$$

$$\approx 1 - |\Gamma'_{ml} - \Gamma_{ml}|^2 (1 + |w_c|^2 - |w_r|^2)$$

$$+ 2 \operatorname{Re} \left[w_c (\Gamma'_{ml} - \Gamma_{ml}) \right]. \tag{10}$$

The uncertainty in F can be written as

$$u(F)^2 \approx 2|w_c|^2 (u^2_{l'} + u^2_l) + 2|\Gamma'_{ml} - \Gamma_{ml}|^2 u(w_c)^2 \tag{11}$$

where we have neglected higher orders in small terms, and where u_l and $u_{l'}$ are the standard uncertainties in the matched loads. They are assumed to be uncorrelated because they correspond to two different matched loads, for different connector types. $u(w_c)$ is the uncertainty in w_c. It is evaluated in the fitting process, and it is not correlated with the uncertainty in $\Gamma'_{ml} - \Gamma_{ml}$. In the examples below, the terms involving $|\Gamma'_{ml} - \Gamma_{ml}|^2$ prove to be negligible, and we are left with

$$u(F) \approx \sqrt{2} |w_c| \sqrt{u^2_l + u^2_{l'}}. \tag{12}$$

The uncertainty in w_r receives both type-A and type-B contributions

$$u(w_r) = \sqrt{u_A(w_r)^2 + u_B(w_r)^2}$$

$$= \sqrt{u_A(w_r)^2 + u_B(w_s)^2 + u_B(w_c)^2} \tag{13}$$

where type-A uncertainties are those evaluated by statistical means, and type-B uncertainties are those evaluated by other means. The type-A uncertainty is evaluated in the course of the fits. The type-B uncertainty in w_c was estimated by performing supplementary measurements on an offset open and offset shorts and quantifying the ripples observed in their corrected reflection coefficients as a function of frequency. The values observed range from $u_B(w_c) = 0.0005|w_r|$ to $0.0015|w_r|$. For the type-B uncertainty in w_s, we first refer to (3) and write

$$w_s = w(\Gamma_{ms}) = \frac{1 - \Gamma_{ms} \Gamma^*_{ml}}{\Gamma_{ms} - \Gamma_{ml}}. \tag{14}$$
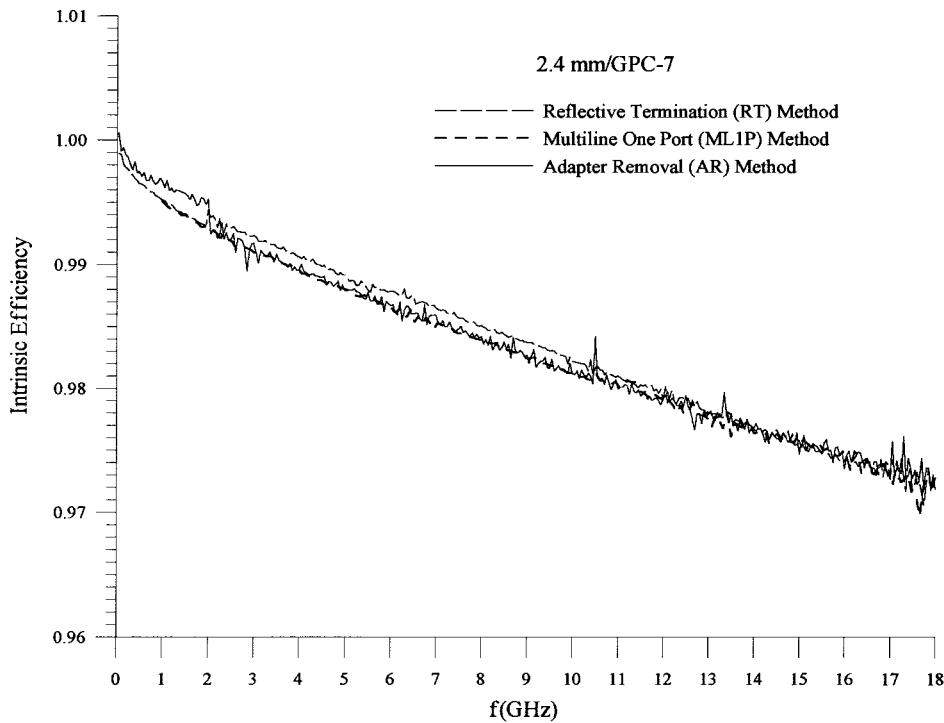
Fig. 6. Comparison of results of three different methods for characterization of a 2.4-mm coaxial to GPC-7 adapter.

Uncertainties in w_s arise due to uncertainties in Γ_{ms} and Γ_{ml}. A small variation $\delta\Gamma_{ml}$ in Γ_{ml} induces a variation in w_r of order $(\delta\Gamma_{ml})^2$ and can, therefore, be neglected. Only a variation in Γ_{ms} contributes to the first-order variation in w_s

$$\delta w_s \approx -\frac{1}{\Gamma_{ms}^2}\delta\Gamma_{ms} \qquad (15)$$

where we have used the facts that $|\Gamma_{ml}|$ is small and $|\Gamma_{ms}|$ is near one. Uncertainties in Γ_{ms} arise from three sources: VNA noise and drift, connector nonrepeatability, and imperfections in the standard short. The corresponding contributions to the standard uncertainty in Γ_{ms} are denoted by e_V, e_c, and e_S. The resulting standard uncertainty in w_s is

$$u_B(w_s) \approx \sqrt{e_V^2 + e_c^2 + e_S^2} \qquad (16)$$

where we have used $|\Gamma_{ms}| \approx 1$. Inserting (16) into (13) yields

$$u(w_r) = \sqrt{u_A(w_r)^2 + e_V^2 + e_c^2 + e_S^2 + u_B(w_c)^2}. \qquad (17)$$

The uncertainty in w_s' is treated in the same manner, yielding a similar equation. Equations (12), (17), and the primed equivalent of (17) are then used in (9) to compute the combined uncertainty in the intrinsic efficiency in the ML1P method.

We must still estimate the different components contributing in (12) and (16). Provided that the VNA has first been allowed to warm up, we have found that it is stable within about 0.0002 over a half day, $e_V = e_V' = 0.0002$. The uncertainty in the short was neglected in the preceding subsection, but since the ML1P uncertainties are somewhat smaller, we retain it here. We estimated e_S from calculations of the loss in coaxial shorts. The values range from 0.0004 for GPC-7 to 0.0007 for 2.4

mm. The connector variability was considered in the preceding subsection, where we adopted $e_c = 0.001$, which we use here as well. The uncertainty in the matched load varies with connector type and frequency. Representative values are 0.001 for GPC-7 and 0.005 for 2.4 mm above 20 GHz. Combining all these contributions typically leads to a type-B uncertainty of about 0.002–0.003. In the examples below, the type-A uncertainties are usually less than 0.001, leading to a typical combined standard uncertainty of 0.002–0.003.

C. AR Technique

The AR technique is described in [6]. It uses a full two-port calibration on each side of the adapter, followed by a measurement through a reference adapter of known electrical length, which is used to establish a phase relation between the two VNA ports. The full S-matrix of the adapter is measured with this method, and the intrinsic efficiency is computed from (1). The uncertainties in this method have not been explicitly evaluated. For good adapters, the uncertainty in the intrinsic efficiency will be dominated by the uncertainty in $|S_{21}|^2$. We use the manufacturer's uncertainties for $|S_{21}|^2$, using the larger of the two values corresponding to the two different connector types in the one-port calibrations. For the adapters considered below, the standard (1σ) uncertainties range from about 0.003 for the GPC-7/WR-62 adapter to 0.012 for the 2.4-mm/WR-28 adapter. The inclusion or exclusion of joint loss in this method is a complicated issue, which we do not address here.

III. RESULTS

A number of different adapters have been characterized using the three methods discussed above. Both coax/waveguide
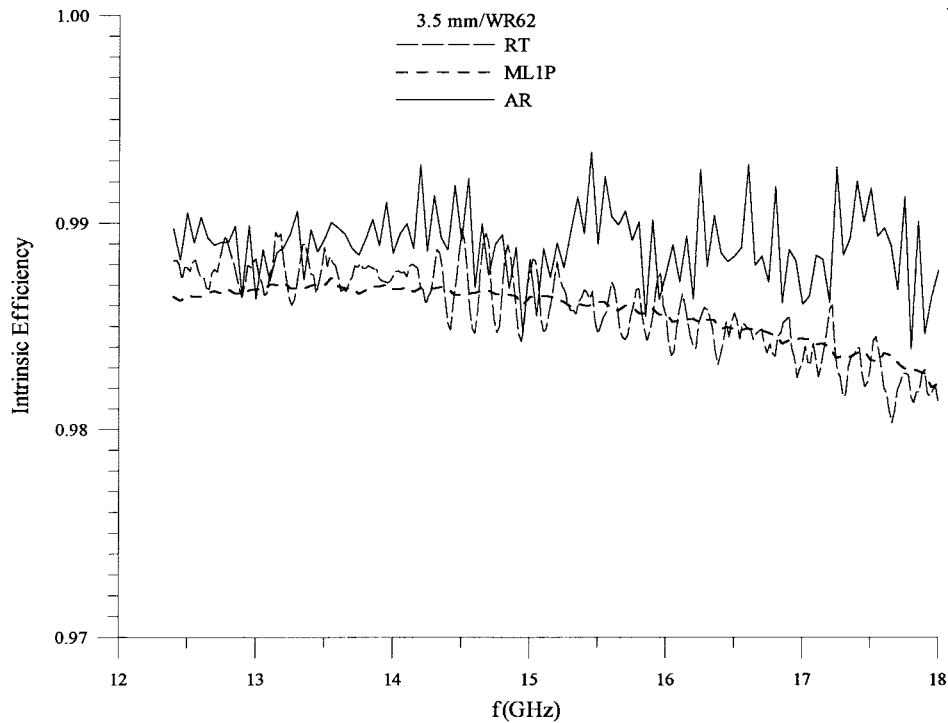
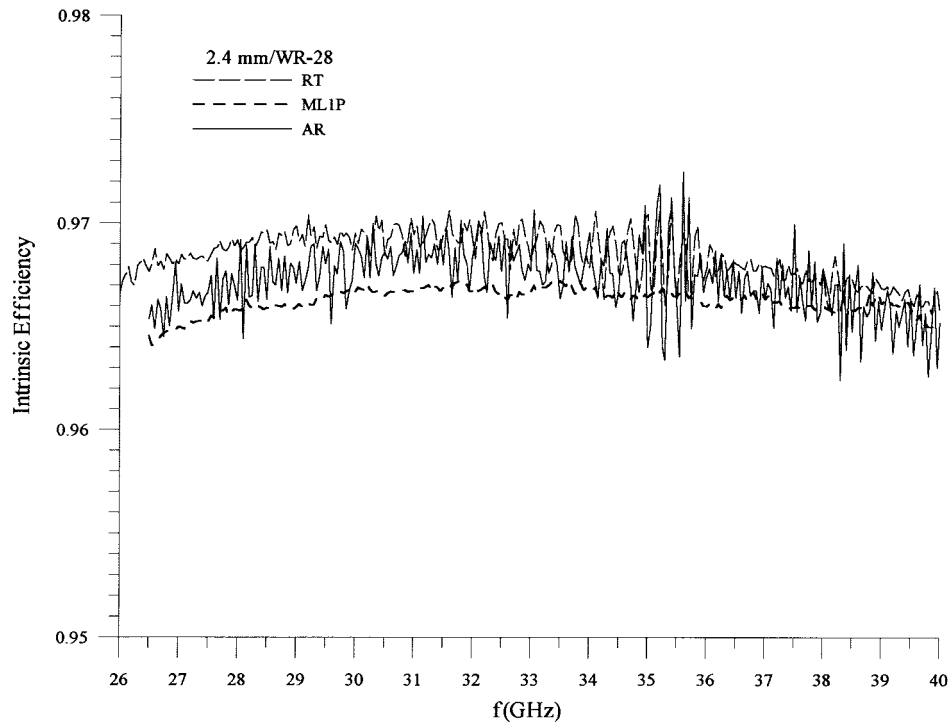Fig. 7. Comparison of results for intrinsic efficiency of a 3.5-mm coaxial to WR-62 waveguide adapter.

Fig. 8. Comparison of results for a 2.4-mm coaxial to WR-28 waveguide adapter.

and coax/coax adapters have been characterized, and in the case of coax/waveguide two different basic adapter designs (tuning stubs and steps) were used. Results for four representative cases are presented here.

The first is an adapter between 2.4-mm coax and GPC-7 coax. Fig. 6 shows the intrinsic efficiency of the adapter obtained with each of the three methods up to 18 GHz,

the maximum frequency for GPC-7. The agreement among the results for the three different methods is excellent. The differences among the three methods are of the order of 0.001 or 0.002, considerably less than the estimated uncertainties, which are about 0.003 for RT, about 0.002 for ML1P, and about 0.003–0.005 for AR, depending on the frequency.
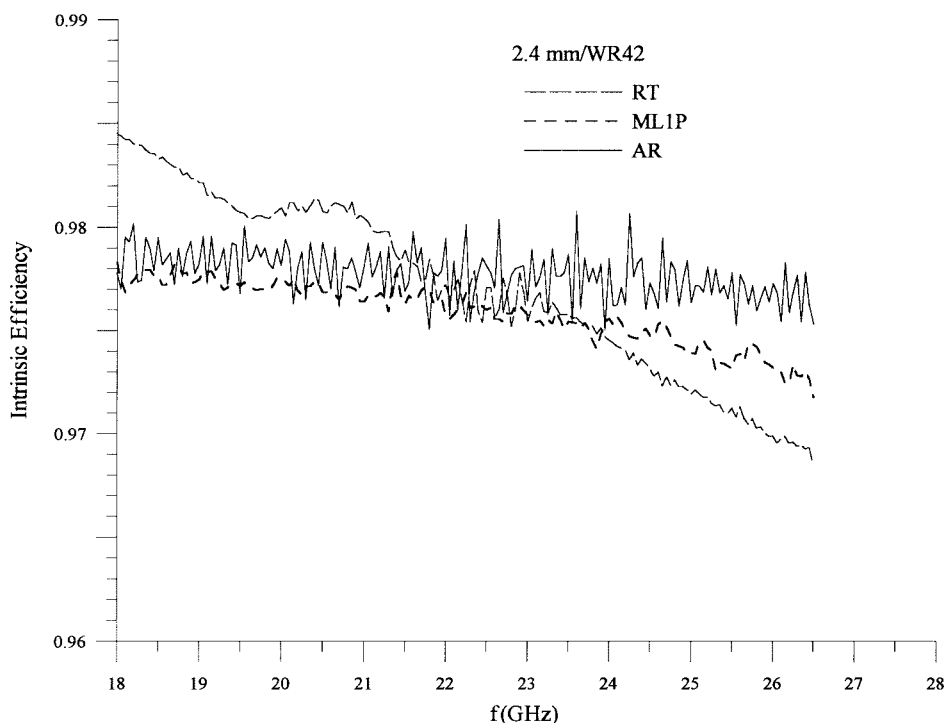
Fig. 9. Worst disagreement among results of three methods encountered thus far.

The second example is an adapter between 3.5-mm coax and WR-62 waveguide. Results obtained with each of the three methods are shown in Fig. 7 for the WR-62 frequency range of 12.4–18 GHz. The agreement among the three methods is quite good, although the AR results are rather noisy, and the agreement deteriorates near the upper frequency limit. The uncertainties are about 0.005 for RT, about 0.002 for ML1P, and about 0.006 for AR. Again, the results of all three methods agree within the estimated uncertainties.

Fig. 8 shows the results for each of the three methods for an adapter between 2.4-mm coax and WR-28 waveguide. The frequency range is the WR-28 band of 26.5–40 GHz. Again, the results of the three methods are all in very good agreement. The maximum discrepancy occurs at the low end of the frequency range and is a little less than 0.004. The uncertainties in this case are 0.005 for RT, 0.003 for ML1P, and 0.012 for AR.

The final example we present is the worst case that we have encountered thus far. It is an adapter between 2.4-mm coax and WR-42 waveguide, and the results are shown in Fig. 9. The ML1P method and the AR method agree well up to about 24 GHz and differ by less than about 0.004 throughout the band. The RT method, however, is about 0.007 above the other two methods at the bottom of the frequency band and about 0.007 below the AR method at the top of the band. This difference is large enough to be worrisome, and further investigation might identify and remedy the cause. The standard uncertainties in this case are 0.005 for RT, about 0.003 for ML1P, and about 0.005 (up to 20 GHz) or 0.012 (above 20 GHz) for AR. Although Fig. 6 does not look good, the discrepancies among the three methods are consistent with

the uncertainties, and this is the worst disagreement we have encountered thus far.

IV. DISCUSSION

Results of all three adapter characterization methods agree within their estimated uncertainties for all the adapters measured thus far. Although the methods differ in their inclusion or exclusion of joint loss, effects of this difference were not evident in the measurements and are probably smaller than the uncertainties. We detected no pattern to the discrepancies that were present. The worst disagreement occurred for a coaxial-to-waveguide adapter in the 18–26.5-GHz frequency range. Very good results were obtained for similar adapters at both higher and lower frequencies.

Each of the methods has its own advantages and disadvantages. The RT method is the quickest and easiest to use, requiring the fewest measurements and relatively little analysis. It does not measure the scattering parameters of the adapter, however, and it assumes the adapter is reciprocal and has low loss. The ML1P method appears to achieve the smallest uncertainties and measures the full scattering matrix. Since it is a one-port method, it assumes that $S_{12} = S_{21}$. It is measurement intensive, especially if a precalibration is performed, and it requires more data analysis than the other methods. Also, its uncertainty analysis could be improved. The adapter-removal method measures the full scattering matrix without having to assume reciprocity, and the analysis is prepackaged. Its drawbacks are that it is measurement intensive, and its uncertainties are somewhat larger than the other methods. It also is susceptible to additional errors due to cable movement and multiple connect–disconnects.

ACKNOWLEDGMENT

REFERENCES

[1] J. Randa, W. Wiatr, and R. L. Billinger, "Comparison of methods for adapter characterization," in *IEEE MTT-S Int. Microwave Symp. Dig.*, Anaheim, CA, June 1999, pp. 1881–1884.

[2] W. C. Daywitt, "Determining adapter efficiency by envelope averaging swept frequency reflection data," *IEEE Trans. Microwave Theory Tech.*, vol. 38, pp. 1748–1752, Nov. 1990.

[3] S. Pucic and W. C. Daywitt, " Single-port technique for adapter efficiency evaluation," in *45th ARFTG Conf. Dig.*. Orlando, FL, May 1995, pp. 113–118.

[4] W. Wiatr, "A method for embedding network characterization with application to low-loss measurements," *IEEE Trans. Instrum. Meas.*, vol. IM-36, pp. 487–490, June 1987.

[5] _____, "A broadband technique for one-port VNA calibration and characterization of low-loss two-ports," in *Precision Electromag. Meas. Conf. Dig.*, Washington, DC, July 1998, pp. 432–433.

[6] "Measuring noninsertable devices," Hewlett-Packard Company, Santa Rosa, CA, Product Note 8510-13, Aug. 1988.

[7] J. Randa, "Uncertainties in NIST noise-temperature measurements," NIST, Boulder, CO, NIST Tech. Note 1502, Mar. 1998.

[8] W. C. Daywitt, "A simple technique for investigating defects in coaxial connectors," *IEEE Trans. Microwave Theory Tech.*, vol. MTT-35, pp. 460–464, Apr. 1987.

[9] J. R. Juroshek, "A study of measurements of connector repeatability using highly reflecting loads," *IEEE Trans. Microwave Theory Tech.*, vol. MTT-35, pp. 457–460, Apr. 1987.

[10] J. Juroshek, C. M. Wang, and G. P. McCabe, "Statistical analysis of network analyzer measurements," *CalLab*, May/June 1998, pp. 26–33.

[11] *ISO Guide to the Expression of Uncertainty in Measurement*. Geneva, Switzerland: Int. Org. Standard., 1993.

[12] B. N. Taylor and C. E. Kuyatt, "Guidelines for evaluating and expressing the uncertainty of NIST measurement results," NIST, Gaithersburg, MD, NIST Tech. Note 1297, Sept. 1994.

Wojciech Wiatr (M'97) received the M.Sc. and Ph.D. degrees in electronics engineering from the Warsaw University of Technology, Warsaw, Poland, in 1970 and 1980, respectively.

His professional career has been spent in microwave metrology. In 1971, he joined the Institute of Electron Technology, Warsaw, Poland, where he was involved in the characterization of semiconductor devices. Since 1972, he has been with the Institute of Electronics Fundamentals (now the Institute of Electronic Systems), Warsaw University of Technology, where he is currently an Assistant Professor. His main scientific work is focused on scattering and noise parameter measurements of active devices, transistors, and monolithic microwave integrated circuits (MMIC's). He has developed the ML1P VNA calibration technique and introduced the multistate radiometry, a novel noise method for the simultaneous determination of small-signal and noise parameters of active devices. He has published one book and approximately 60 papers, and holds two patents.

Robert L. Billinger received the Associates degree in electronics technology from Wichita Technical Institute, Wichita, KS, in 1979.

From 1979 to 1984, he was with PureCycle Corporation, where he became Manager of Electronic Production and Test. Since 1985, he has been with the Radio-Frequency Technology Division, Radio-Frequency Electronics Group, National Institute of Standards and Technology (NIST), Boulder, CO, where he is involved in the area of thermal noise.

J. Randa (M'84–SM'91) received the Ph.D. degree in physics from the University of Illinois at Urbana-Champaign, in 1974.

He then successively held post-doctoral or faculty positions at Texas A&M University, University of Manchester (U.K.), and the University of Colorado at Boulder. During this time, he performed research on the phenomenology of elementary particles and on theories of fundamental interactions. Since 1983, he has been with the Radio-Frequency Technology Division, National Institute of Standards and Technology (NIST), Boulder, CO. From 1983 to early 1994, he was in the Fields and Interference Metrology Group, where he was involved in the characterization of electromagnetic environments, probe development, and other topics in EMI metrology. He is currently in the Radio-Frequency Electronics Group, NIST, where he works in the area of thermal noise.